Turkish Journal of Electrical Engineering & Computer Sciences

http://journals.tubitak.gov.tr/elektrik/

Research Article

Turk J Elec Eng & Comp Sci
(2018) 26: 234 – 244

doi:10.3906/elk-1611-210

Usage of segmentation for noise elimination in reconstructed images in digital holographic interferometry

Gülhan USTABAŞ KAYA*, Zehra SARAÇ
Department of Electrical and Electronics Engineering, Faculty of Engineering, Bülent Ecevit University, Zonguldak, Turkey

Received: 22.11.2016 • **Accepted/Published Online:** 13.07.2017 • **Final Version:** 26.01.2018

Abstract: In this paper, we propose to enhance the image in digital holography by using an artificial neural network and an iterative algorithm with Nakamura's approach based on segmentation. It is well known that reconstructed three-dimensional (3D) images suffer from noise in digital holography. In addition, obtaining 3D reconstructed images takes a long time due to large pixel numbers in reconstructed images and lack of memory in the system. The segmentation process is an application that overcomes these problems. Therefore, we focus on the implementation of segmentation for image enhancement. In addition, the results of the segmentation process for both methods are compared in terms of image enhancement. Later, the relative errors are calculated.

Key words: Noise reduction, segmentation, reconstructed image, artificial neural network

1. Introduction

The noise reduction of reconstructed images for image enhancement is one of most important topics in digital image processing, and it has opened up new horizons for developing current research. It has been conducted in every field, such as ultrasound imaging [1], analysis of medical images [2], optical coherence tomography [3], visualization of radar images [4], and digital holography techniques [5].

Due to the fact that holographic images suffer from Gaussian, Poisson, Erlang (gamma), salt and pepper, uniform, intensity, and/or speckle noises, most applications are introduced in the literature in order to improve the image quality of digital holographic images [6–10]. Gerchberg and Saxton calculated the phase of diffraction to obtain noiseless images in 1971 [11]. Later, implementing a low-pass filter and median filter to reconstruct three-dimensional (3D) images and using multiple polarization holograms were introduced by Rong et al. for noise reduction [12]. In addition, an iterative algorithm, implemented with a phase retrieval process, was proposed by Nakamura et al. to obtain a high image quality in reconstructed 3D images [13]. Moreover, noise filtering (2D FIR filter) in an ultrasound image application [14], an image processing algorithm for high-resolution satellite images with the use of artificial neural networks (ANNs) [15,16], and a denoising technique using a feedforward artificial neural network [17] have been employed for image enhancement.

As mentioned above, ANNs have been used to enhance reconstructed images in digital holography [18]. However, while holographic images are training with ANNs, many problems such as large pixel numbers and a lack of memory in the system occur. To overcome these problems, an image segmentation process in ANNs can

*Correspondence: gulhan.ustabas@beun.edu.tr

be used [19]. This process can be implemented for noise reduction, as well. Different types of segmentation, namely pixel-based, point-based, edge-based, region-based, and threshold-based, have been developed to date [20]. The threshold method, which is one of the most powerful segmentation techniques for images with light objects on a dark background, can specifically be used. To determine the best threshold values, the histogram approach is applied. Furthermore, the histogram is calculated to choose the best pixel value, i.e. the one that occurs at the highest frequency.

Although image segmentation is an important process for removing noise, it cannot produce the desired result in some digital image processing applications. Therefore, we have focused on this process to implement it in the ANN and in the iterative algorithm that was proposed by Nakamura et al. for the first time [13]. This method is called Nakamura's approach (NA). Moreover, these methods are compared in terms of image enhancement.

This paper is organized into four sections. Section 2 includes theoretical fundamentals of the NA and ANN methods. The multilayer perceptron (MLP) network [21], which is a type of ANN network, is also used in the study. In addition, implementations of the segmentation process to both methods are described. In Section 3, a comparison of the MLP network and NA method with the segmentation process is given. The 3D perspectives for intensity distribution of reconstructed images for both methods are also shown in this section. In addition, relative errors are calculated to substantiate the results of the 3D perspective.

2. Theoretical fundamentals

2.1. NA method

The NA method is a method of phase determination for enhancing the image in digital holography. With this method, a noiseless image is obtained by calculation of an unknown phase sign. Although the phase value is already calculated, it is not known whether the phase sign is positive or negative. To determine the phase sign, two different image sensors are used and two different hologram recordings are performed at the same time.

The first sensor is used to record the hologram pattern obtained from reference and object waves. In Eq. (1), the hologram intensity pattern can be mathematically defined [13].

$$I_1(x,y) = A(x,y)^2 + A_r(x,y)^2 + 2A(x,y)A_r\cos\{\varphi(x,y) - \varphi_r(x,y)\} \tag{1}$$

Here, (x,y) represents the coordinates of the image plane. In addition, $A(x,y)$ defines the complex amplitude of an object and $A_r(x,y)$ gives the complex amplitude of the reference wave, which is a plane wave. $\phi(x,y) = (\varphi(x,y) - \varphi_r(x,y))$ identifies the angle between the object and reference waves.

The complex amplitude of the object wave can be defined as $K(x,y) = A(x,y)\exp(i\varphi(x,y))$, and the complex amplitude of the reference wave can be given as $K_r(x,y) = A_r(x,y)\exp(i\varphi(x,y))$ [13].

The second sensor is also used to record the intensity distribution of the object wave in this study and is defined mathematically by Eq. (2).

$$I_2(x,y) = A(x,y)^2 \tag{2}$$

The phase information of the hologram is gained by using Eq. (1) and Eq. (2), as given in Eq. (3).

$$\phi(x,y) = \cos^{-1}\left(\frac{I_1(x,y) - I_2(x,y) - A_r(x,y)^2}{2\sqrt{I_2}A_r(x,y)}\right) \tag{3}$$

The image enhancement and phase sign calculation are achieved in four steps. By taking an inverse Fresnel propagation of complex amplitude for the object wave (K) in the hologram plane, the complex amplitude for the object wave (T) in the 3D object plane is calculated in the first step. K_n is given as the nth estimated complex amplitude of the object wave. To obtain a single image, an adaptive filter is used in the spatial frequency domain when there is a twin image in the complex area. The region of the 3D image is removed by cleaning the twin image and thus the second step is finished. From the extracted twin image, the complex amplitude of the 3D object is expressed as T'. In the third step, Fresnel propagation is applied to move from the object layer to the hologram layer. The complex amplitude (K') in the hologram plane is calculated by Fresnel propagation. By calculating the phase of the complex amplitude, the phase sign is also identified in the last step. Whether this sign and the sign of the complex amplitude of the initial hologram are the same or not can then be compared. The iteration is stopped if they are the same. If not, iteration continues until the two signs are the same. The block diagram of the used iterative algorithm in this method is shown in Figure 1 [13].

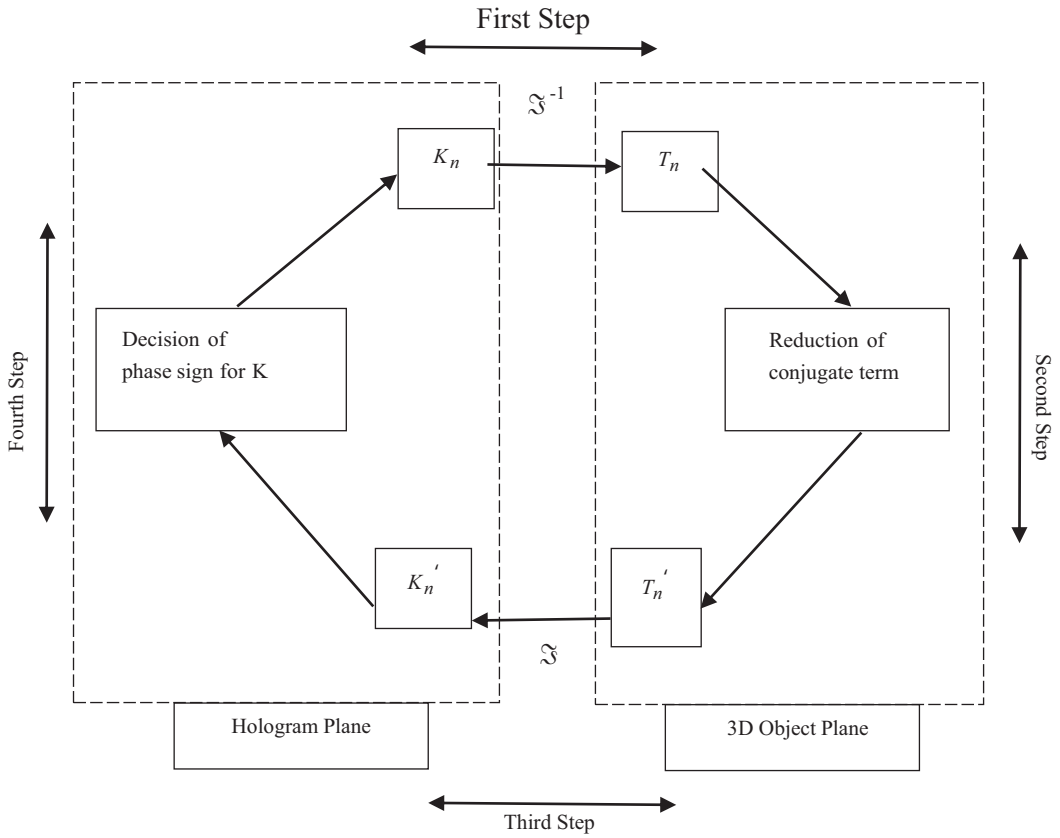

Figure 1. Block diagram of the iterative algorithm.

2.2. Multilayer perceptron (MLP) network

ANNs, which are called connectionist and parallel-distributed systems, are computational paradigms based on mathematical models. The possible problems during the connections are reduced in the training process by distributing the configuration of weighting with the ANN [19]. To train the network and minimize the squared error between network output and target output values, we use the backpropagation algorithm.

MLP is used to create the ANN architecture, since its structure is simple and sufficient in learning and training large datasets. It is also helpful to solve the problems that constitute linear and nonlinear applications. The possible problems in the MLP network are reduced during the training process. It consists of an input layer, hidden layer, and output layer. This network aims to achieve a balance between the input and target output data in the input layer and output layer, respectively [22]. In our study, one hidden layer is used for the MLP network, and this network is shown in Figure 2.

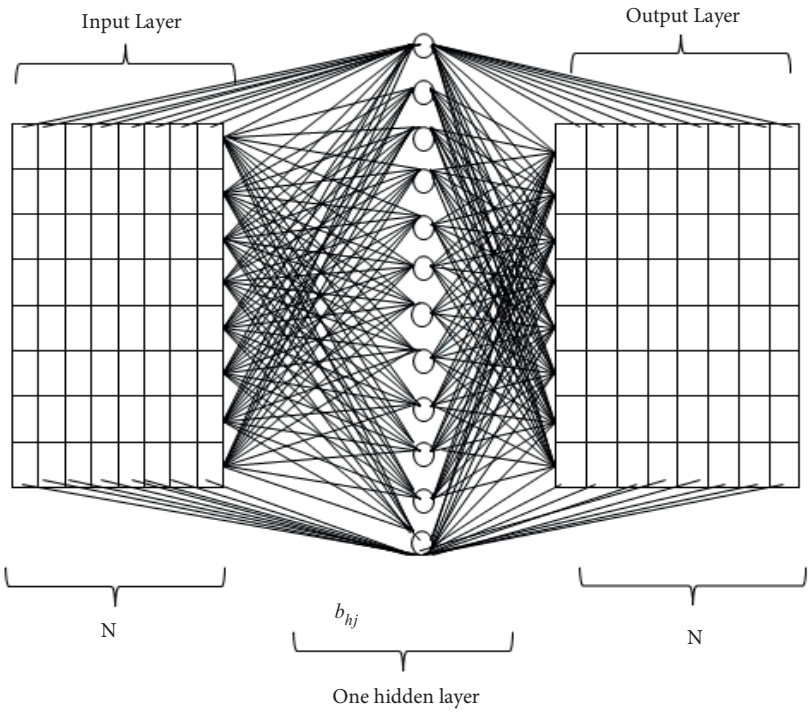

Figure 2. Multilayer perceptron network model with one hidden layer.

The layers of the constituted architecture completely connect with each other. The neurons are located at each layer. By using weighted connections, the information of the neurons is transferred forward from node to node according to the desired outputs via backpropagation algorithms.

The system is trained by using input and output data. Before updating the weights, the error value between the input and output data is backpropagated to the hidden neurons. The errors are already minimized after specific iteration. The MLP network output is calculated with Eq. (4), using one hidden layer.

$$y = f_0 \left\{ \sum_{k=1}^{m} f_h \left(\sum_{j=1}^{n} w_{hj} x_j + b_{hj} \right) w_{ok} + b_{ok} \right\} \tag{4}$$

Here, x_j is defined as the input parameter and y is given as the output parameter. The activation function of the hidden layer and output layer are identified as f_0 and f_h, respectively. The weights of the hidden input layer, the biases of the hidden layer, the weights of the hidden output layer, and the biases of the output layer are given as w_{hj}, b_{hj}, w_{ok}, and b_{ok}, respectively.

The general idea of using MLP in this study is to reduce noise in the holographic images. The reconstructed holographic image is obtained with a Fourier transform algorithm. This matrix array of the reconstructed image is used for the input layer dataset.

The hidden layer neurons consist of one or more layers. This layer is based on the training process. As for the target output image in the output layer, it is obtained from the Gerchberg–Saxton algorithm after 10 iterations [11].

2.3. Segmentation process with the MLP network

Many problems occur while holographic images are being trained with ANNs. The most significant ones are large pixel numbers and a lack of memory in the system. Thus, we need to do another operation before processing the output and input data. The compression and decompression processes must be applied to the used data. Basic methods to compress the image data are the processes of segmentation of the pixels and rasterization. If the compressed image has a large pixel number, achievement of the training process is too difficult. Therefore, the process of splitting up the large image into subimages is necessary. The input images can be split up into subvectors of 8 × 8, 4 × 4, or 2 × 2 pixels. This process is also called segmentation. In this study, the applied segmentation process for image enhancement is performed by using a bilinear interpolation method with 0.35 ratio scaling instead of splitting up subvectors because the reconstructed image has a big pixel size of 480 × 640. If the images are split up into subvectors of 8 × 8, 4 × 4, or 2 × 2, the image processing takes a long time, and it causes an increase in the process steps. Therefore, the reconstructed image pixel is resized to a 168 × 224 pixel size with a 0.35 ratio scaling by segmentation process with the bilinear interpolation method.

The resampling process through bilinear interpolation is shown in Figure 3. In addition, the original and scaled-up images are defined by their pixel size in this figure. The configuration of Figure 3 can be defined mathematically as follows [23]:

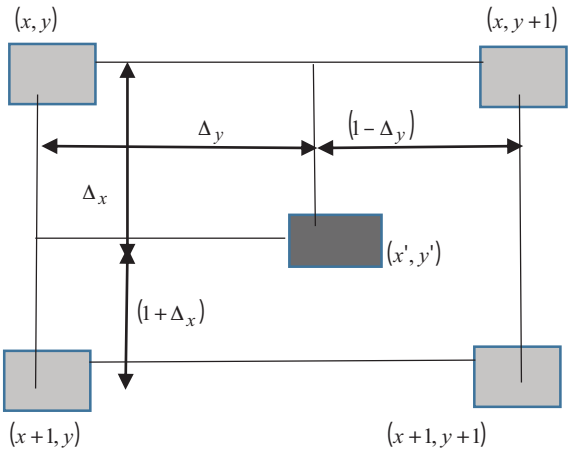

Figure 3. Configuration of the original and resized images.

Here, the original image is expressed as I_1, which has $(X \times Y)$ pixel size. The resized image is defined as I_2, which has $(X' \times Y')$ pixel size.

$$\text{Let } x_f = x' * \frac{X}{X'} \quad \text{for} \quad x' = 1, ..., X' \quad \text{and} \quad y_f = y' * \frac{Y}{Y'} \quad \text{for} \quad y' = 1, ..., Y'. \tag{5}$$

Here, (x_f, y_f) is defined as pairs of each point in I_1 image.

Let $x = |x_f|$ and $y = |y_f|$. In addition, let:

$$\Delta_x = x_f - x \text{ and } \Delta_y = y_f - y \tag{6}$$

The scaled-up image is defined mathematically in Eq. (7).

$$I_2(x', y') = I_1(x, y) * (1 - \Delta_x) * (1 - \Delta_y) + I_1(x + 1, y) * \Delta_x * (1 - \Delta_y) + I_1(x, y + 1) * (1 - \Delta_x) * \Delta_y + I_1(x + 1, y + 1) * \Delta_x * \Delta_y \quad (7)$$

The reason for choosing a scaling ratio of 0.35 is to obtain the best calculated histogram. As is well known, the thresholding method is the simplest method for image segmentation. This method is based on a threshold value that turns a gray-scale image into a binary image. One way of finding the best threshold value is to employ a histogram approach, which is an important tool in image analysis. To find the proper histogram in this study, the reconstructed image pixel is resized with a scaling of different ratios such as 0.10 and 0.35, respectively.

To explain why the scaling ratio chosen is 0.35, the histograms are given in Figures 4a and 4b with different scaling ratios. It is obvious from the histogram given in Figure 4b that the scaling ratio of 0.35 has a more homogeneous distribution.

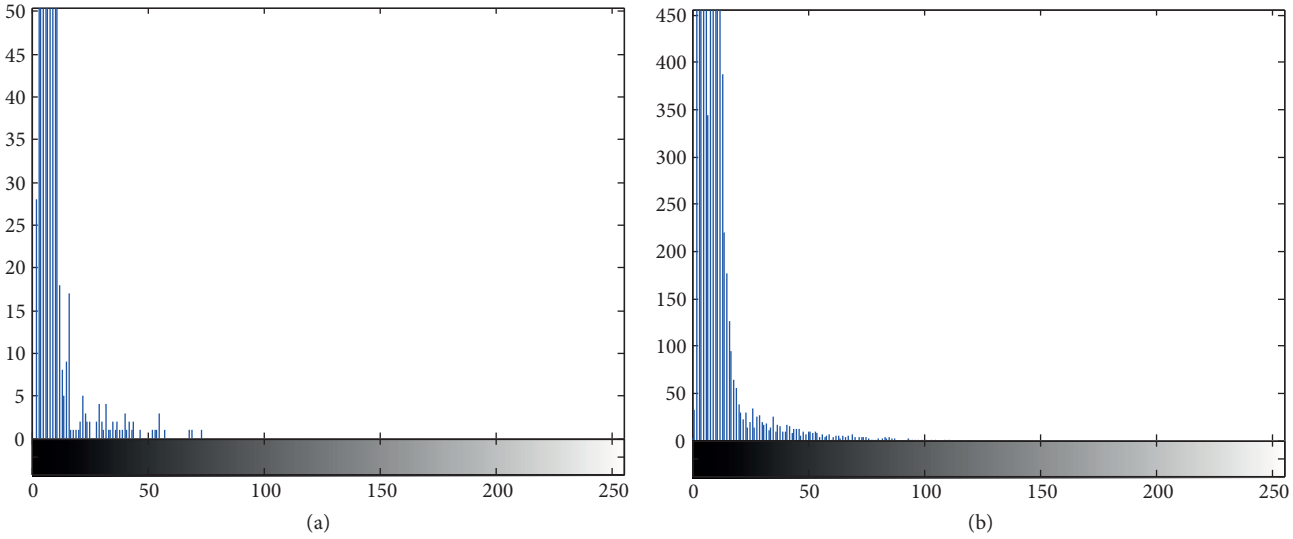

Figure 4. Error histograms of different scaling ratio: a) 0.10 scaling ratio, b) 0.35 scaling ratio.

In addition, this resized image is used as an input parameter in the segmentation method of the ANN. After the segmentation process, rasterization must be done. When the subimage is in 2D form, it is converted into 1D form by rasterization. The 1D form is a vector whose length is N. To obtain the real size of images, by using decompression, the similar inverse process must be done.

3. Segmentation process with the NA method

Not only is image segmentation one of the applications in ANNs, but it also has an important place in applications of digital image processing for noise reduction. Therefore, we can implement the segmentation process with the NA method. To make an accurate comparison of the MLP network and the NA method, the reconstructed image pixel is resized at a 0.35 ratio scaling, which is the same ratio as the MLP network. The plotted histogram is given in Figure 5 for the threshold value in the segmentation process.

Although it is desired that the noise of the image be eliminated at a high degree with the segmentation process, image enhancement using the NA method with segmentation cannot be adequately achieved. To show the effect of the segmentation processes in both methods, comparison results are given in Section 3.

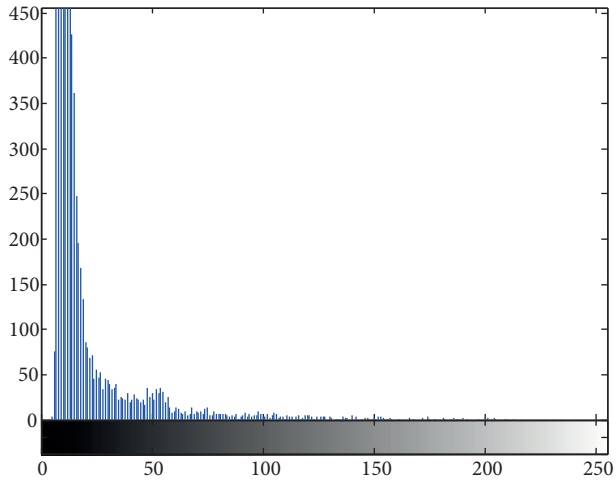

Figure 5. Error histograms obtained by using segmentation with the NA method.

4. Results

In this section, we evaluate the effect of the segmentation process on the MLP network and the NA method by making a comparison of the image enhancement of the reconstructed 3D images in digital holography. The MLP network with segmentation is the first implemented method to be used in comparing the process and the NA method with segmentation is the second implemented method in this study.

The performance criterion called the mean squared error (MSE) is calculated after the training process of the MLP network to determine the numbers of hidden layer neurons. Because we obtain a defective image after using 12 neurons, the number of hidden layer neurons is chosen as 12 according to calculated MSE values. The training MSE values of the MLP network according to different numbers of hidden neurons are given in the Table.

Table. Training MSE values of the MLP network according to different numbers of hidden neurons.

Number of hidden neuron layers	MSE values of MLP
4	5.12006e-04
6	4.13796e-04
8	4.14498e-04
10	4.14496e-04
12	4.09697e-04
14	1.27063e-03
16	2.93290e-03
18	2.12113e-03

To show noise reduction by using the MLP network with segmentation for star and dice images (Figures 6a–6d), respectively, the obtained reconstructed 3D images are given in Figures 6a and 6c. In addition, their 3D perspectives for intensity distributions are shown in Figures 6b and 6d. Moreover, the obtained reconstructed 3D images with the NA method with segmentation are presented for star and dice images and the 3D perspectives for intensity distributions of these images are presented in Figures 7a–7d.

Although the noise of the reconstructed image cannot be adequately eliminated by using the NA network with segmentation, it is noticeably decreased with the use of the MLP network with segmentation. In addition,

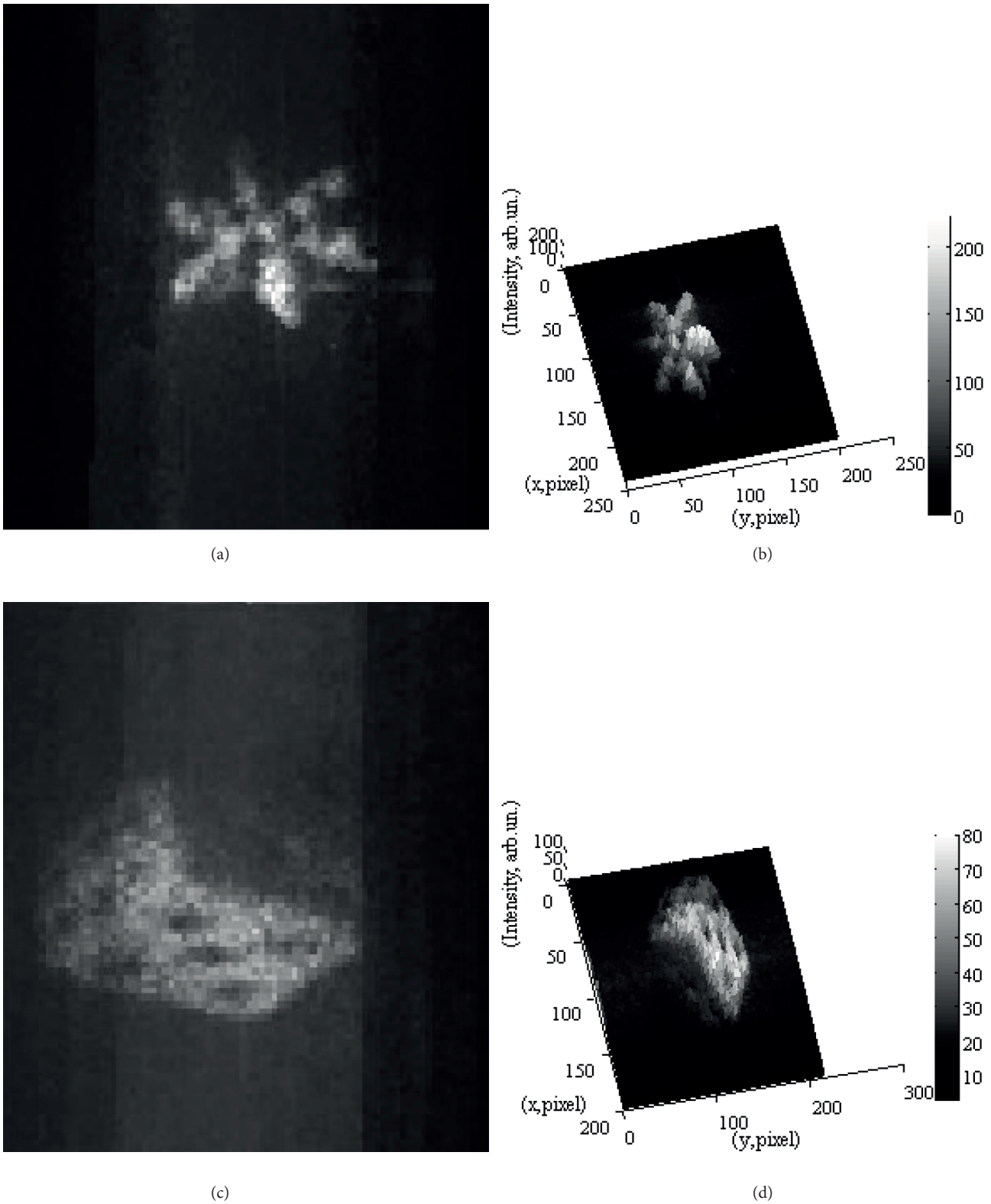

(a) (b)

(c) (d)

Figure 6. 3D reconstructed images obtained with the MLP network and their 3D perspectives for intensity distribution: a) 3D reconstructed star image, b) 3D perspective for intensity distribution of Figure 6a, c) 3D reconstructed dice image, d) 3D perspective for intensity distribution of Figure 6c.

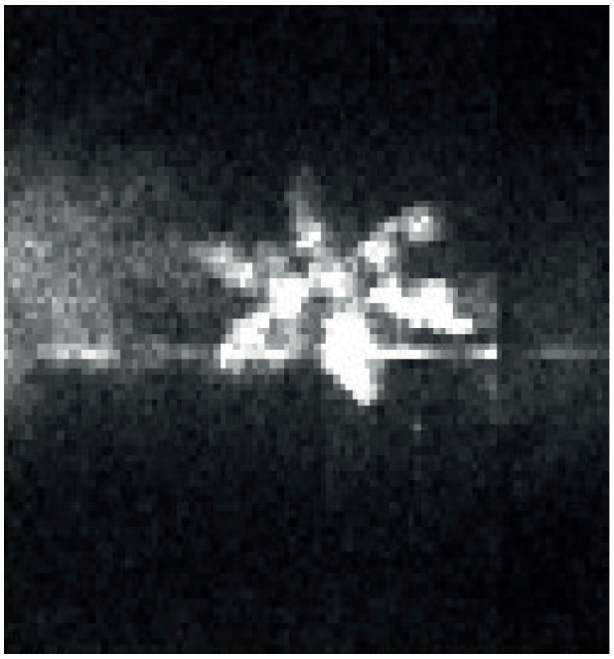

(a)

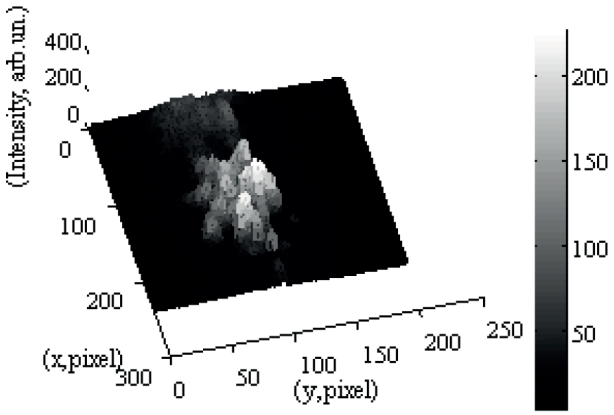

(b)

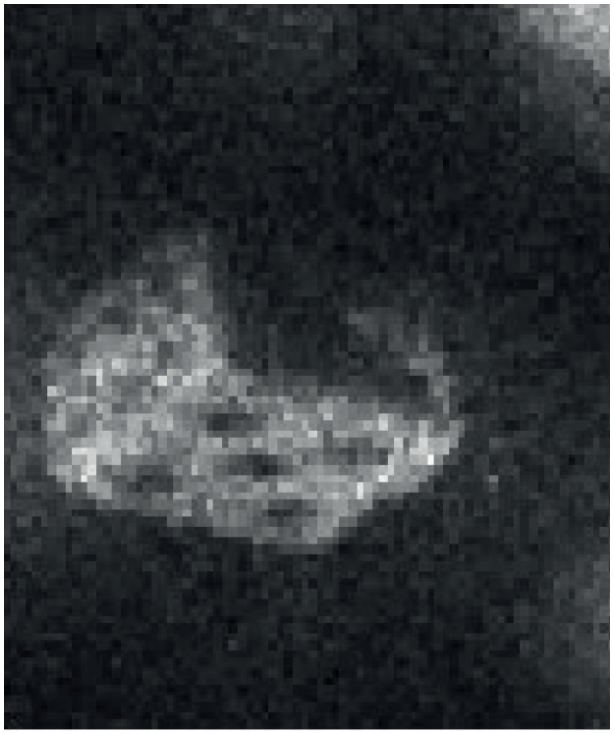

(c)

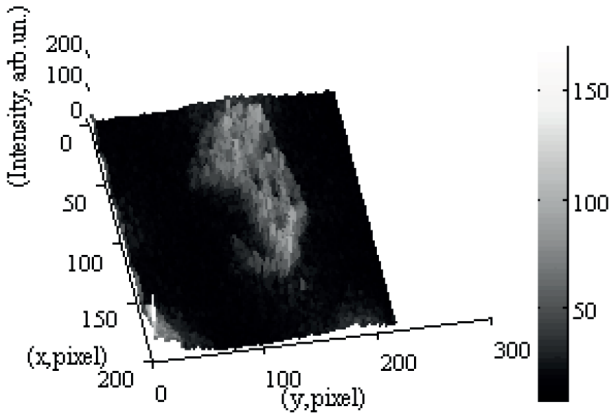

(d)

Figure 7. 3D reconstructed images obtained with the NA method and their 3D perspectives for intensity distribution: a) 3D reconstructed star image, b) 3D perspective for intensity distribution of Figure 7a, c) 3D reconstructed dice image, d) 3D perspective for intensity distribution of Figure 7c.

it seems that in Figure 6 that image enhancement of the reconstructed images can be achieved by the MLP network with segmentation.

Not only are 3D perspectives for intensity distributions of the results given in this study, but the numerical calculations for noise elimination of the reconstructed 3D images are also provided, as achieved by MATLAB. Therefore, relative errors are calculated for both methods by using the reconstructed images obtained with and without the segmentation process. First, the relative errors of star and dice images are calculated for the MLP network and are found to be 89% and 41%, respectively. These ratios show that the resemblance between the reconstructed images of the MLP network and MLP network with segmentation differs greatly because the reduction of noise with the segmentation process resulted in a noiseless image. Second, the relative errors of star and dice images are calculated for the NA method. They are found to be 52% and 22%, respectively. These values are smaller than the values obtained with the MLP network (89% and 41%).

5. Conclusion

The segmentation process has been implemented for the ANN method and digital image processing applications in recent studies, but no study has yet aimed to eliminate noise in reconstructed 3D images in digital holography. To enhance the reconstructed 3D image in digital holography, the implementation of the segmentation process to the MLP network and the NA method is proposed here for the first time. The purpose of this proposal is to overcome the problem that has come into existence in cases with large pixel numbers and lack of memory during image processing on a computer. Therefore, the MLP network and the NA method with segmentation process are compared in terms of image quality by obtaining the 3D perspectives for intensity distributions. The obtained results are presented in Figures 6b and 6d for the MLP network and in Figures 7b and 7d for the NA method with segmentation process, respectively. Figures 6b and 6d indicate that the MLP network with segmentation process can produce a result with fairly low noise. To support the results of the 3D perspective for the intensity distribution of star and dice reconstructed images, relative errors are calculated for both methods. These errors are found to be 89% and 41% for the MLP network and 52% and 22% for the NA method, respectively. Within this context, it should be emphasized that the segmentation method produces a better result for noise reduction with the MLP network than with the NA method. In conclusion, the comparison process of the MLP network and the NA method with segmentation shows that the desired image with minimum noise is obtained by using the MLP network with segmentation.

References

[1] Cronan JJ. Ultrasound: is there a future in diagnostic imaging? Journal of the American College of Radiology 2006; 3: 645-646.

[2] Maini R, Aggarwal H. A comprehensive review of image enhancement technique. J Comput 2010; 2: 8-13.

[3] Podoleanu AG. Optical coherence tomography. Brit J Radiol 2005; 78: 976-988.

[4] Sarode MV, Deshmukh PR. Reduction of speckle noise and image enhancement of images using filtering technique. International Journal of Advancements in Technology 2011; 2: 30-38.

[5] Abdelsalam DG, Kim D. Coherent noise suppression in digital holography based on flat fielding with apodized apertures. Opt Express 2011; 19: 17951-17959.

[6] Kaur S. Noise types and various removal techniques. International Journal of Advanced Research in Electronics and Communication Engineering 2015; 4: 226-230.

[7] Kaisar S, Rijwan S, Al Mahmud J, Rahman MM. Salt and pepper noise detection and removal by tolerance based selective arithmetic mean filtering technique for image restoration. International Journal of Computer Science and Network Security 2008; 8: 271-278.

[8] Mythili C, Kavitha V. Efficient technique for color image noise reduction. Research Bulletin of Jordan 2011; 2: 41-44.

[9] Cai X, Wang H. The influence of hologram aperture on speckle noise in the reconstructed image of digital holography and its reduction. Optics Communication 2008; 281: 232-237.

[10] Cai X. Reduction of speckle noise in the reconstructed image of digital holography. Optik 2010; 121: 394-399.

[11] Gerchberg RW, Saxton WO. A practical algorithm for the determination of phase from image and diffraction plane pictures. Optik 1972; 35: 237-246.

[12] Rong L, Xiao W, Pan F, Liu S, Li R. Speckle noise reduction in digital holography by use of multiple polarization holograms. Chin Opt Lett 2010; 8: 653-655.

[13] Nakamura T, Nitta K, Matoba O. Iterative algorithm of phase determination in digital holography for real-time recording of real objects. Appl Optics 2007; 46: 6849-6853.

[14] Latifoglu F. A novel approach to speckle noise filtering based on artificial bee colony algorithm: an ultrasound image application. Comput Meth Prog Bio 2013; 111: 561-569.

[15] Farnood Ahmadi F, Valadan Zoej MJ, Ebadi H, Mokhtarzade M. The application of neural networks, image processing and cad-based environments facilities in automatic road extraction and vectorization from high resolution satellite images. International Archives of the Photogrammetry, Remote Sensing and Spatial Information Sciences 2008; 37: 585-592.

[16] Zurada JM. Introduction To Artificial Neural Systems. Bristol, UK: West Publication Company, 1992.

[17] Saikia T, Sarma KK. Multilevel-DWT based image de-noising using feed forward artificial neural network. In: IEEE 2014 International Conference on Signal Processing and Integrated Networks; February 2014; Delhi, India. New York, NY, USA: IEEE. pp. 791-794.

[18] Nayak R, Jain L, Ting B. Artificial neural networks in biomedical engineering: a review. In: Proceedings of the 1st Asian-Pacific Congress on Computational Mechanics; 2001. Amsterdam, the Netherlands: Elsevier Science Limited. pp. 887-892.

[19] Chandhok C. A novel approach to image segmentation using artificial neural networks and K-means clustering. International Journal of Engineering Research and Applications 2012; 2: 274-279.

[20] Agravat H, Rathod K. Classification of different segmentation methods for handwritten words. Research Hub-International Multidisciplinary Research Journal 2015; 2: 1-4.

[21] Duda RO, Hart PE, Stork DG. Pattern Classification. 2nd ed. New York, NY, USA: Wiley Publishing, 2000.

[22] Isa IS, Saad Z, Omari S. Suitable MLP network activation functions for breast cancer and thyroid disease detection. In: IEEE 2010 Second International Conference on Computational Intelligence, Modelling and Simulation; 28–30 September 2010; Tuban, Indonesia. New York, NY, USA: IEEE. pp. 39-44.

[23] Chang KT. Computation for Bilinear Interpolation. Introduction to Geographic Information Systems. 5th ed. New York, NY, USA: McGraw-Hill, 2009.